Research Note

Mesoporous sodalite: A novel, stable solid catalyst for base-catalyzed organic transformations

Ganapati V. Shanbhag, Minkee Choi, Jeongnam Kim, Ryong Ryoo *

Center for Functional Nanomaterials and Department of Chemistry, Graduate School of Nanoscience and Technology, Korea Advanced Institute of Science and Technology, Daejeon 305-701, Republic of Korea

ABSTRACT

Mesoporous sodalite with a mesoporous/microporous hierarchical structure was successfully synthesized using an organosilane surfactant. It showed about 10-fold high surface area and 4-fold large pore volume, as compared with sodalite with solely microporous structure. The basicity of MPSOD was higher than that of CsNaX or KAlMCM-41. The catalytic activities of this mesoporous zeolite were evaluated for various base catalyzed reactions involving bulky and small substrates, *viz.* Knoevenagel condensation, Claisen–Schmidt condensation in liquid phase, and acetonylacetone cyclization in vapor phase. The catalyst showed higher activity and longer lifetime than CsNaX and KAlMCM-41.

© 2009 Elsevier Inc. All rights reserved.

1. Introduction

The potential applications of heterogeneous base catalysts in specialty and fine chemical production have expanded significantly over the years [1–6]. Base-catalyzed condensation, addition, and isomerization reactions are some of the important steps for building large and complex molecules for the synthesis of many fine chemicals and pharmaceutical products. Basic solids such as Cs-ZSM-5 and MgO have been used as catalysts in industrial processes due to their activity, thermal stability, and reusability [7,8]. While metal ion-exchanged zeolites possess basic sites of relatively low strength, they can be easily regenerated from poisoning by air, as compared with strong solid bases, such as alkaline earth oxides [9]. Nevertheless, applications of basic zeolites are limited by slow diffusion of substrates into their micropores for bulky molecular reactions and rapid deactivation due to coke formation [10]. In principle, alkali metals can be ion exchanged onto MCM-41-like mesoporous aluminosilicate for application as a basic catalyst for bulky substrates. However, mesoporous materials built with amorphous frameworks have serious drawbacks due to weak basicity and low hydrothermal stability. Stronger basicity can be induced in materials like mesoporous aluminosilicates and metal-organic

frameworks by modifications such as covalent grafting of amines and impregnation of basic metal oxides [11–16]. However, such modified catalysts also carry limitations such as low hydrothermal stability and leaching of active species, preventing them from finding practical applications.

Among the various strategies to synthesize mesoporous zeolites, very few were successful in obtaining high crystallinity with tunable mesoporosity. In one such work, Choi et al. reported a direct synthesis route to mesoporous zeolites with a tunable mesoporous structure using amphiphilic organosilane surfactants as a mesopore-directing agent [17]. The mesoporous MFI zeolite thus synthesized exhibited much higher catalytic activities for the conversion of bulky molecules than a conventional MFI zeolite, providing evidence that the catalytic conversion occurred at the mesopore walls [18]. In catalytic reactions involving small molecules, these two kinds of zeolites initially showed no significant difference, but the mesoporous zeolite exhibited remarkably improved catalytic lifetimes. However, the successful catalytic application has mostly been limited to high silica mesoporous MFI zeolites, which are useful for acid-catalyzed reactions. It is therefore of interest to develop a high aluminum-containing mesoporous zeolite with a basicity similar to the existing basic zeolites. Sodalite is a zeolite with high aluminum content (Si/Al = 1) and high stability in basic solution. However, it thus far has not found any significant catalytic applications due to its inaccessible cages with small pore openings (2.8 Å).

---

* Corresponding author. Fax: +82 42 350 8130.
 E-mail address: rryoo@kaist.ac.kr (R. Ryoo).

In the previous works, we had successfully synthesized mesoporous zeolites and zeolite-type solids such as MFI, BEA, LTA, and AlPO via direct hydrothermal assembly methods [17–21]. In this study, we report a new basic solid catalyst, *viz.* mesoporous sodalite with high aluminum content and highly crystalline zeolitic walls. This basic mesoporous zeolite was synthesized using an amphiphilc organosilane surfactant, followed by ion exchange with K$^+$. The catalytic activity was compared with that of a basic alkali-exchanged NaX and NaAlMCM-41 (Si/Al = 1) for reactions involving bulky and small substrates. The K$^+$-exchanged mesoporous sodalite has been studied in detail, since K$^+$ salts are inexpensive and have better exchange ability than Cs$^+$ salts. The mesoporous sodalite was tested in C–C bond-forming reactions in liquid phase, which involved bulky substrates. Knoevenagel condensation is a key step in the preparation of several pharmaceutics including the antimalarial drug lumefantrine, whereas Claisen–Schmidt condensation products such as 2′-hydroxychalcone and flavanone derivatives are used in the synthesis of anti-inflammatory, anti-allergic, and anti-cancer drugs [22,23]. The catalyst has been further tested in vapor phase intramolecular aldol condensation of acetonylacetone to form a cyclopentenone derivative as the major product. Cyclopentenone derivatives are used as intermediates in the synthesis of perfumes and antibiotics [24].

2. Experimental

2.1. Synthesis of catalysts

A highly crystalline mesoporous sodalite was synthesized by mixing an organosilane [(CH$_3$O)$_3$SiC$_3$H$_6$N(CH$_3$)$_2$C$_{16}$H$_{33}$]Cl (51.5 wt% methanol solution) with sodium metasilicate (Na$_2$SiO$_3$.9H$_2$O), sodium aluminate (53% Al$_2$O$_3$, 43% Na$_2$O), NaOH, and H$_2$O to achieve a gel composition of 1.7 SiO$_2$/15 Na$_2$O/1 Al$_2$O$_3$/80 H$_2$O/0.3 organosilane in mole ratio. The gel was heated at 423 K for 6 h in a tumbling autoclave for precipitation of sodalite. The zeolite product was collected by filtration, and washed with hot distilled water until the pH of the filtrate was neutral. The product was then dried and calcined in air at 823 K. This sample is designated by MPSOD. Another sample of mesoporous sodalite was synthesized with a gel composition of 1.5 SiO$_2$/20 Na$_2$O/1 Al$_2$O$_3$/160 H$_2$O/0.5 organosilane, by following the same hydrothermal procedure as MPSOD except for 373 K. This sample was denoted as MPSOD-1. A third sample of sodalite was synthesized by the same procedure as for MPSOD, except that the organosilane surfactant was not used. This sample without mesoporosity is denoted as SOD. NaAlMCM-41 with Si/Al = 1 was synthesized according to the procedure reported elsewhere [25]. NaX zeolite was procured from Aldrich.

2.2. Cation exchange of catalysts

Cation exchange of Na-form of all the catalyst samples was performed with 0.5 M chloride solutions of K$^+$ or Cs$^+$. One gram of the powder was stirred with 10 ml of the solution at 353 K for 3 h. The resultant mixture was then cooled to RT, filtered, and washed repeatedly with distilled water until it was free from Cl$^-$ and physisorbed metal ions. This procedure was performed three times in all to ensure maximum cation exchange. The resulting exchanged materials, i.e., K$^+$-exchanged MPSOD (hereafter KMPSOD), K$^+$-exchanged microporous sodalite (KSOD), KAlMCM-41, and CsNaX, were dried at 403 K for 12 h. They were subsequently calcined in static air at 773 K for 4 h except for KAlMCM-41 (containing template), which was calcined by a previously reported procedure [26]. Besides, as synthesized AlMCM-41 was used for cation exchange since the calcined sample was not stable under the applied experimental conditions.

2.3. Catalyst characterization

X-ray diffraction (XRD) patterns were recorded with a Rigaku Multiflex diffractometer equipped with Cu $K\alpha$ radiation (40 kV, 40 mA). The textural properties of the samples were measured by N$_2$ sorption at liquid nitrogen temperature with a Quantachrome AS-1MP volumetric adsorption analyzer. Samples were dried at 573 K in a dynamic vacuum for 2 h before the N$_2$ physisorption measurements. The specific surface area was determined using the standard BET method on the basis of adsorption data. The pore size distributions were calculated from both the adsorption and desorption branches of the isotherms using the BJH method and the Kelvin equation. Elemental analyses were performed by inductively coupled plasma spectroscopy (ICP) using an OPTIMA 4300 DV (Perkin–Elmer) instrument. Nitrogen content was measured by an elemental analyzer, EA-110 (Thermo Finnigan). Transmission electron micrograph (TEM) images were obtained with a Tecnai G2 F30 microscope at an operating voltage of 300 kV. Scanning electron microscopy (SEM) was conducted using a Hitachi S-4800 microscope operating at 2 kV without a metal coating. ^{27}Al MAS–NMR spectra were recorded on a Bruker AM-300 NMR spectrometer (see Supplementary information (hereafter SI) for details). Basicity measurements were carried out by TPD of adsorbed CO$_2$ using a Belcat-M instrument (see SI).

2.4. Catalytic activity measurements

Knoevenagel condensation of 4-isopropylbenzaldehyde (4-IPB) with ethylcyanoacetate (ECA) was carried out in a Pyrex reactor equipped with a reflux condenser (Eyela Chemistation) under a N$_2$ atmosphere to prevent the oxidation of aldehyde. No solvent was used in the reaction. In a typical reaction, 10 mmol of 4-IPB and 10 mmol of ECA were mixed with 0.05 g of catalyst and stirred at 353 K. The products were analyzed by an Acme 6100 gas chromatograph fitted with a flame ionization detector and a HP-1 capillary column.

Claisen–Schmidt condensation of 2′-hydroxyacetophenone (2-HAcPh) with benzaldehyde was carried out in a Pyrex reactor under N$_2$ atmosphere. Five millimole of 2-HAcPh and 10 mmol of benzaldehyde were heated at 423 K with 0.05 g of the catalyst. After the reaction, the reaction mixture was diluted with 2 ml of THF to confirm the dissolution of all the components, and was then analyzed as described above.

Vapor phase cyclization of acetonylacetone (AcAc) was conducted in a fixed bed, down flow reactor using 0.5 g of catalyst pellets (20–35 mesh). The catalyst was pre-activated in a flow of air at 773 K for 2 h, and then cooled down to the reaction temperature. High purity N$_2$ (30 ml min^{-1}) was used as a carrier gas. The feed (AcAc) was vaporized before passing into the reactor. The product was analyzed with an Acme 6100 gas chromatograph fitted with Supelco α-Dex225 capillary column. Products of all the above-mentioned reactions were identified with authentic samples and GC combined with mass spectroscopy.

3. Results and discussion

3.1. Catalyst characterization

The percentage compositions of different metal ions present in the catalyst are listed in Table 1. Nitrogen content was measured by elemental analysis, and the result indicated that the N-containing groups (from the organosilane) were completely removed by the work-up and calcination steps. Wide angle XRD patterns of MPSOD and MPSOD-1 consisted of peaks that were typical of microporous sodalite (Fig. 1B). The two prominent peaks at

Table 1
Physicochemical properties of the catalysts.

Catalyst	Si/Al[a]	M[+] content[a] (mol%)			S_{BET} (m^2 g^{-1})	Vp[b] (ml g^{-1})
		Na	K	Cs		
MPSOD	1.1	100	–	–	193	0.42
MPSOD-1	1.0	100	–	–	850	1.12
KMPSOD	1.1	26	74	–	182	0.38
KSOD	1.0	85	15	–	19	0.10
KAlMCM-41	1.1	05	95	–	310	0.32
CsNaX	1.2	47	–	53	350	0.19

[a] Determined by ICP analysis.
[b] Total pore volume obtained at P/Po = 0.95.

$2\theta = 13.9°$ and $24.3°$ represented (110) and (211) crystal planes, respectively. XRD peak widths of mesoporous sodalite samples were markedly broader than those of ordinary sodalite crystals, which indicated a highly nanocrystalline nature of the framework. Among the two mesoporous sodalite samples, MPSOD-1 showed much broader XRD peaks, signifying that the material was built with a thin sodalite framework. Notably, MPSOD-1 exhibited a single broad peak in the low-angle XRD pattern [Fig. 1A(a)], indicating a higher structural correlation in the mesopore arrangement. The XRD pattern of KMPSOD suggested that the sodalite structure was retained after ion exchange and calcination steps [Fig. 1B(c)].

N$_2$-sorption measurements of MPSOD and MPSOD-1 samples exhibited type IV isotherms with a H1-type hysteresis loop, which was typical of mesoporous solids (Fig. 1C). Table 1 represents the structural and textural properties of the materials. The higher specific surface area and larger pore volume were attributed to the presence of highly mesoporous structures in the MPSOD and MPSOD-1. The KMPSOD catalyst showed about 10-fold higher surface area (182 m^2 g^{-1}) and 4-fold larger pore volume (0.38 ml g^{-1}) than KSOD (19 m^2 g^{-1} and 0.1 ml g^{-1}). A small decrease in the surface area of MPSOD after ion exchange was attributed to an increase in the weight of the sample when Na$^+$ ions were replaced with K$^+$.

TEM images [Fig. 2(a) and (b)] revealed that both MPSOD and MPSOD-1 possessed disordered mesoporous structures. The MPSOD-1 sample was built with a much thinner framework (2.5 nm) than the MPSOD sample (8 nm). The thin framework of MPSOD-1 provided the highest surface area and pore volume among the three sodalite samples. Unfortunately, this thin framework collapsed under the reaction conditions generating water as a by-product. Therefore, in the following catalytic investigations, we focused on the MPSOD sample which possessed high surface area as well as sufficiently high stability. SEM images of KMPSOD revealed the presence of particles of spherical morphology with an average diameter of 1 μm, much smaller than that of KSOD [Fig. 2(c) and (d)].

^{27}Al solid state MAS NMR spectra of MPSOD-1 and KMPSOD in a fully rehydrated state after calcination at 823 K are depicted in Fig. S2 (SI). The ^{27}Al NMR spectra show two peaks. A peak at ~55 ppm is the tetrahedral Al signal. The second peak appearing at ~0 ppm with lower intensity is assigned to the octahedral Al in the form of extra-framework species or the framework Al species located at the defect sites. The spectra of MPSOD-1 and KMPSOD contained a major peak at 55 ppm and a negligibly small peak at 0 ppm, which indicated that most of the Al atoms were located inside the zeolite framework.

CO$_2$ is often used as a probe molecule in TPD due to its small size, good thermal stability, and weak acidic character. The amount of desorbed CO$_2$ and the temperature of maximum desorption of CO$_2$ are the criteria for the concentration and strength of basic sites, respectively. The basicity data of the catalysts are presented in Fig. 1D. While the total basicity of MPSOD after K$^+$ exchange remained unchanged (109 μmol g^{-1}), the basic strength increased as expected. The temperature of peak maximum of CO$_2$ desorption indicated that the basic strength of KMPSOD was greater than that of KAlMCM-41 (553 and 473 K, respectively). The intrinsic basicity of porous materials depends on the framework oxygen atoms bearing negative charges. The electron density on these oxygen atoms is a measure of basic strength, which depends on porous structure, nature of cations, and their location. Al sites of KAlMCM-41 are located on amorphous mesopore walls, whereas in KMPSOD they are situated mostly on crystalline mesopore walls. It is worth noting that the temperature of peak maximum for KMPSOD (553 K) was slightly higher than that of CsNaX (508 K).

3.1.1. Catalytic activity study

Knoevenagel condensation of 4-IPB with ECA is catalyzed by mild basic catalysts. The activity of KMPSOD was compared with that of KAlMCM-41 and CsNaX which contained similar Si/Al ratios but differed in pore size, pore structure, and basicity. The activity and selectivity of the catalysts are listed in Table S1 (SI). KMPSOD was the most active catalyst (78%) followed by MPSOD (70%), KAlMCM-41 (46%), and CsNaX (35%) after 1 h reaction. The higher activity of KMPSOD was attributed to the basic sites located in
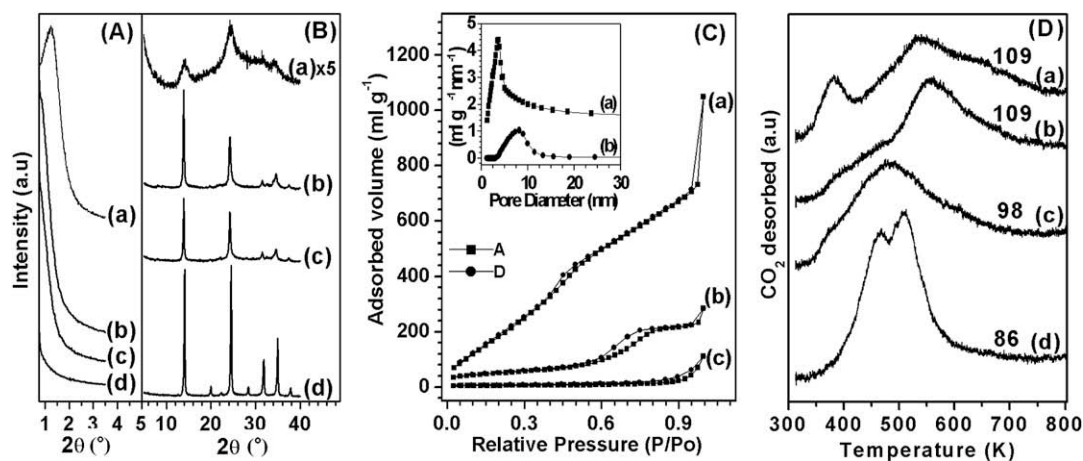

Fig. 1. (A) Low-angle and (B) wide angle XRD patterns: (a) MPSOD-1, (b) MPSOD, (c) KMPSOD, and (d) KSOD. (C) N$_2$ sorption isotherms: (a) MPSOD-1, (b) KMPSOD, and (c) KSOD. Inset: Pore size distribution. (D) TPD profiles of CO$_2$ desorption: (a) MPSOD, (b) KMPSOD, (c) KAlMCM-41, and (d) CsNaX. The data on each plot represent the total basicity in μmol g^{-1}.
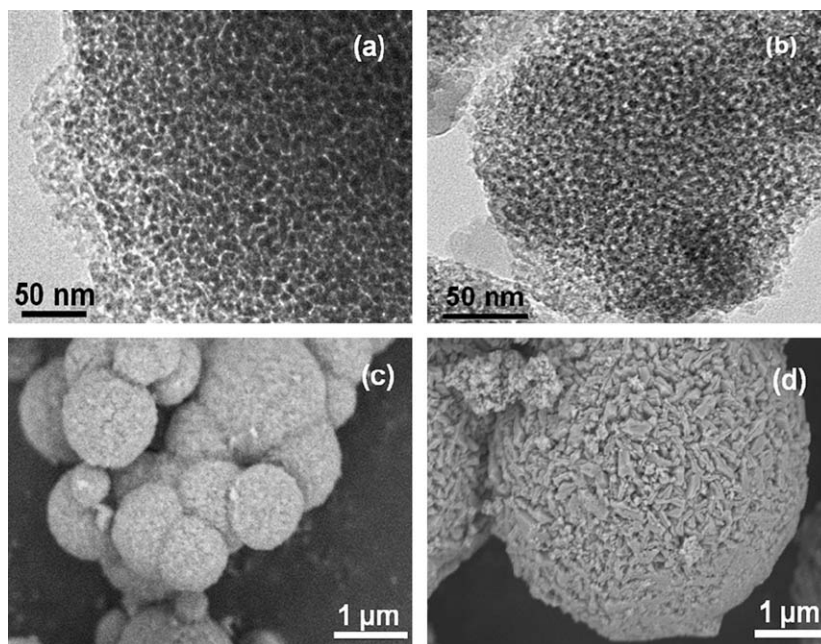
Fig. 2. TEM images: (a) MPSOD, and (b) MPSOD-1. SEM images: (c) KMPSOD, and (d) KSOD.

their mesopores, which facilitated the diffusion of bulky molecules. On the other hand, CsNaX showed comparatively low activity, as expected, since the bulky product should be formed not at the basic sites located inside the cavities, but preferentially at the sparse sites situated on the zeolite external surface. KAlMCM-41 showed a higher activity than CsNaX, but its structure collapsed as a result of the water produced during the reaction, as evident by XRD. Although KAlMCM-41 contained a high number of basic sites (Si/Al = 1.1), it exhibited a poor hydrothermal stability, whereas KMP-SOD showed a good recyclability and retained its structural characteristics even after 3 cycles.

The condensation of 2-HAcPh and benzaldehyde involves Claisen–Schmidt condensation in the first step to yield 2′-hydroxychalcone, followed by isomerization and ring closure to give flavanone. This reaction requires a catalyst having moderate basicity. KMPSOD showed high activity (67% conversion) and good selectivity for flavanone (52%) after 5 h of reaction, exceeding CsNaX and KAlMCM-41 as shown in Table S2 (SI). The higher activity of KMPSOD in this case is due to its mesoporous structure as well as moderate basicity. KAlMCM-41 though contains mesopores, its lower activity can be attributed to its relatively weak basicity.

Solid base-catalyzed vapor phase condensation of AcAc involves intramolecular aldol condensation and cyclization to give 3-methyl-2-cyclopenten-1-one (ketone) as the major product and 2,5-dimethylfuran (ether) as the minor product. Apart from commercial importance, this reaction is also studied to identify the basicity present in the catalyst containing acid base pairs [27]. The reaction was carried out in a down flow reactor at 623 K with WHSV 1.9 h^{-1}. This reaction also involves smaller organic molecules that are easily formed and diffused through the micropores of large pore zeolites such as CsNaX. The blank experiment gave 5% conversion with 0% selectivity for ketone at 1 h. The KMPSOD catalyst converted 91% of AcAc into products: ketone (88%) and ether (4%) at 2 h. The high selectivity for ketone reflected the basic character of KMPSOD, since the product, ketone, was formed by base catalysis [27]. All the catalysts exhibited some level of deactivation, which was evident by a loss in the conversion with time on stream. During the initial period of reaction (at 1 h), the activities of KMPSOD and CsNaX were almost the same (~90%) (Fig. 3).
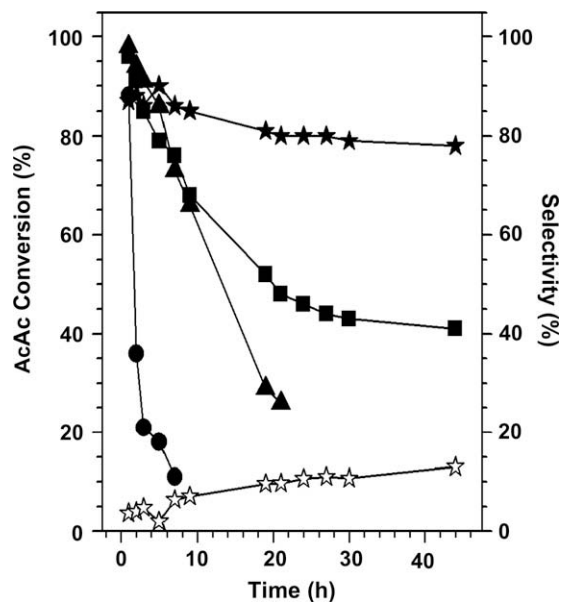

Fig. 3. Vapor phase condensation of acetonylacetone with different catalysts. Conversion: KMPSOD (■), CsNaX (●), and KAlMCM-41 (▲). Selectivity obtained with KMPSOD: ketone (★) and ether (☆). *Reaction conditions*: temperature = 623 K, WHSV = 1.9 h^{-1}.

While KMPSOD showed a slow deactivation with time (conversion decreased to 75% in 7 h), the activity of CsNaX decreased rapidly with time (conversion dropped to 11% in 7 h). The retention of activity of mesoporous sodalite for a longer period can be attributed to the facile diffusion of the products from its mesopores. In contrast, for microporous zeolites, such as CsNaX, the organic compounds undergo side reactions, leading to coke formation inside the channels which blocks the active sites. Moreover, the activity of KAlMCM-41 decreased rapidly than that of KMPSOD. The KAlMCM-41 catalyst showed a 90% loss of small angle XRD peaks when measured after the reaction. As indicated by this change, the catalytic deactivation of KAlMCM-41 seemed to be due to the

collapse of the mesoporous structure during the water-generating reaction.

4. Conclusions

The mesoporous sodalite investigated in this study contains mesoporous–microporous hierarchical structure. It showed about 10-fold higher surface area and 4-fold larger pore volume than microporous sodalite. The basicity of the mesoporous sodalite was higher than that of CsNaX or KAlMCM-41 when compared under similar Al concentrations. The mesoporous sodalite showed high catalytic activity with good recyclability in liquid phase Knoevenagel condensation and Claisen–Schmidt condensation reactions. It also exhibited high activity and stability toward deactivation in a vapor phase acetonylacetone condensation reaction and therefore could be used for longer reaction time, whereas CsNaX deactivated rapidly due to coke formation. In conclusion, mesoporous sodalite is a stable and versatile basic catalyst for a range of bulky and small molecular reactions. Given its now established physicochemical properties, it can also be used as a stable support for further surface modifications, which will expand its applicability.

Acknowledgement

Appendix A. Supplementary data

Supplementary data associated with this article can be found, in the online version, at doi:10.1016/j.jcat.2009.03.014.

References

[1] M.J. Climent, A. Corma, S. Iborra, J. Primo, J. Catal. 151 (1995) 60.
[2] Y.V.S. Rao, D.E. de Vos, P.A. Jacobs, Angew. Chem. Int. Ed. 36 (1997) 2661.
[3] J. Weitkamp, M. Hunger, U. Rymsa, Microporous Mesoporous Mater. 48 (2001) 255.
[4] F. Figueras, M.L. Kantam, B.M. Choudary, Curr. Org. Chem. 10 (2006) 1627.
[5] X. Liu, H. He, Y. Wang, S. Zhu, X. Piao, Fuel 87 (2008) 216.
[6] Y.X. Feng, N. Yin, Q.F. Li, J.W. Wang, M.Q. Kang, X.K. Wang, Catal. Lett. 121 (2008) 97.
[7] B.S. Beshty, F.P. Gortsema, G.T. Wildman, J.J. Sharkey, US Patent 5231187 (1993), Merck & Co. Inc.
[8] K. Tanabe, W.F. Holderich, Appl. Catal. A. Gen. 181 (1999) 399.
[9] H. Hattori, Chem. Rev. 95 (1995) 537.
[10] S.C. Lee, S.W. Lee, K.S. Kim, T.J. Lee, D.H. Kim, J.C. Kim, Catal. Today 44 (1998) 253.
[11] S. Jaenicke, G.K. Chuah, X.H. Lin, X.C. Hu, Microporous Mesoporous Mater. 35 (2000) 143.
[12] J. Yu, S.Y. Shiau, A.N. Ko, Catal. Lett. 77 (2001) 165.
[13] S. Hasegawa, S. Horike, R. Matsuda, S. Furukawa, K. Mochizuki, Y. Kinoshita, S. Kitagawa, J. Am. Chem. Soc. 129 (2007) 2607.
[14] L. Soldi, W. Ferstl, S. Loebbecke, R. Maggi, C. Malmassari, G. Sartori, S. Yadab, J. Catal. 258 (2008) 289.
[15] Y.K. Hwang, D.Y. Hong, J.S. Chang, S.H. Jhung, Y.K. Seo, J. Kim, A. Vimont, M. Daturi, C. Serre, G. Férey, Angew. Chem. Int. Ed. 47 (2008) 4144.
[16] J. Gascon, U. Aktay, M.D. Hernandez-Alonso, G.P.M. van Klink, F. Kapteijn, J. Catal. 261 (2009) 75.
[17] M. Choi, H.S. Cho, R. Srivastava, C. Venkatesan, D.H. Choi, R. Ryoo, Nat. Mater. 5 (2006) 718.
[18] V.N. Shetti, J. Kim, R. Srivastava, M. Choi, R. Ryoo, J. Catal. 254 (2008) 296.
[19] M. Choi, R. Srivastava, R. Ryoo, Chem. Commun. (2006) 4380.
[20] R. Srivastava, M. Choi, R. Ryoo, Chem. Commun. (2006) 4489.
[21] D.-H. Lee, M. Choi, B.-W. Yu, R. Ryoo, Chem. Commun. (2009) 74.
[22] U. Beutler, P.C. Fuenfschilling, A. Steinkemper, Org. Process Res. Dev. 11 (2007) 341.
[23] S. Hatziieremia, A.I. Gray, V.A. Ferro, A. Paul, R. Plevin, Br. J. Pharmacol. 149 (2006) 188.
[24] J. Mathew, US Patent 5026918 (1991), Petrolite Corp.
[25] M.T. Janicke, C.C. Landry, S.C. Christiansen, S. Birtalan, G.D. Stucky, B.F. Chmelka, Chem. Mater. 11 (1999) 1342.
[26] M.T. Janicke, C.C. Landry, S.C. Christiansen, D. Kumar, G.D. Stucky, B.F. Chmelka, J. Am. Chem. Soc. 120 (1998) 6940.
[27] R.M. Dessau, Zeolites 10 (1990) 205.